Astron. Astrophys. 344, 494–498 (1999)

ASTRONOMY
AND
ASTROPHYSICS

The kinematics of RR Lyrae stars observed by Hipparcos⋆

B. Chen

Departament d'Astronomia i Meteorologia, Universitat de Barcelona, Avda. Diagonal 647, E-08028 Barcelona, Spain

Received 3 July 1998 / Accepted 9 December 1998

Abstract. We discuss the distributions of velocities and metallicities for 144 RR Lyrae stars observed by the *Hipparcos* astrometry satellite. The new absolute magnitude calibration of RR Lyrae stars and an all-sky reddening map have been used to derive individual distances accurately.

Three statistical analysis techniques based on pattern recognition theory are used to seek for significant signatures of stellar population characteristics in the sample. It is found that the intrinsic stellar distributions show a significant departure from a continuous trend, giving evidence for a discrete Galactic thick disk. Our results suggest that the disk and halo are separate kinematic structure without a smooth transition from one to the other.

Key words: methods: data analysis – stars: kinematics – stars: variables: RR Lyr – Galaxy: kinematics and dynamics – Galaxy: stellar content

1. Introduction

RR Lyrae stars are intrinsically bright, and their absolute magnitudes are within a narrow range (Layden 1998). Moreover, they are easily distinguished from the large numbers of foreground disk stars. Thus RR Lyrae stars are considered as good tracers to probe the kinematics of stellar populations and to give insight into the dynamics and evolution of the Galaxy.

Hipparcos observations have provided accurate proper motions for 186 RR Lyrae stars. Fig. 1 shows the distributions in the plane of (σ_π, π). We can see that most stars in our sample have apparent negative parallaxes or $\sigma_\pi/\pi > 100\%$. Only one star (RR Lyrae itself) has $\sigma_\pi/\pi < 20\%$. It is clear that we have to use photometry to obtain their individual distances.

Recently, Fernley et al. (1998), Tsujimoto et al. (1998), Luri et al. (1998), etc. have derived a photometric calibration of the mean absolute magnitudes M_v of RR Lyrae stars from Hipparcos observations. A good convergence is now obtained although there is no agreement as to the exact relation between absolute magnitude and metallicity $[Fe/H]$.

Another important factor in the distance determination of RR Lyrae is interstellar extinction. Previous authors (Fernley et al. 1998; Layden et al. 1996; Luri et al. 1998) used either the Burstein & Heiles (1982) reddening map or the Arenou et al. (1992) extinction model to derive extinction. However the Arenou et al. (1992) extinction model is only good for $r < 1$ kpc, and presents a systematic bias for $r > 1.5$ kpc (Chen et al. 1998). The Burstein & Heiles (1982) reddening map does not cover all the sky. Recently, a new reddening map has been published (Schlegel et al. 1998). This reddening map includes all the sky, and is twice as accurate as the older Burstein & Heiles (1982) reddening estimates in regions of low and moderate reddening. The map is expected to be significantly more accurate in regions of high reddening. Its spatial resolution is about 6.1′. This map is intended to supersede the Burstein & Heiles (1982) map in both accuracy and spatial resolution.

In this paper, we use the newest absolute magnitude calibration and the Schlegel et al. (1998) all-sky reddening map to get the space motions for RR Lyrae stars (Sect. 2). In Sect. 3, the wavelet transform and the kernel density estimation are used to identify intrinsic stellar signatures in the kinematics and metallicity space. In Sect. 4, we use multivariate cluster analysis to disentangle different stellar populations, and investigate the kinematics of these stars in an effort to constrain the main

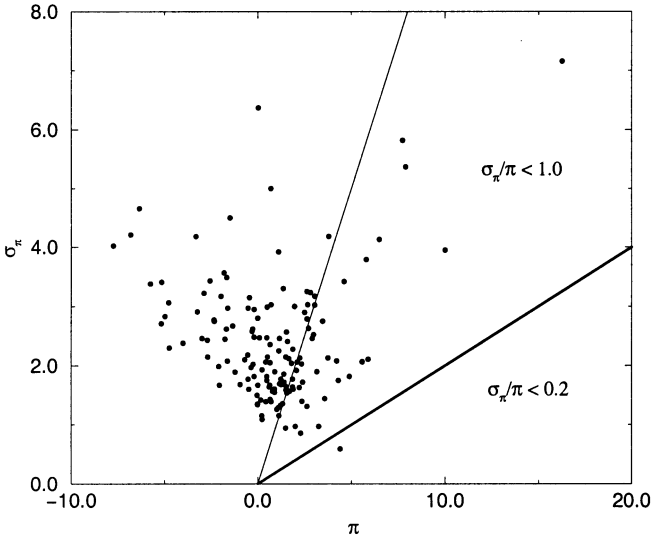

Fig. 1. Distribution of trigonometric parallax error (σ_π) *vs* trigonometric parallax (π) for RR Lyrae stars observed by Hipparcos Astrometry satellite

Send offprint requests to: bchen@mizar.am.ub.es

⋆ Based in part on observations made with ESA Hipparcos astrometry satellite

stellar populations and models of the formation and evolution of the Galaxy.

2. The data

Hipparcos made photometric and astrometric observations for 186 RR Lyrae stars. Of these 186 stars, we have rejected 42 stars which do not have good observations for all observed quantities. The sample (144 stars) used by us is the same as that used by Fernley et al. (1998) for absolute magnitude calibration of RR Lyrae stars. The Galactic latitudes and longitudes for these RR Lyrae stars were obtained from the GCVS (Kholopov 1985).

Several new absolute magnitude calibrations for RR Lyrae stars have been published. Fernley et al. (1998) found

$$M_v = (0.18 \pm 0.03)([\mathrm{Fe/H}]{+}1.53) + (0.77 \pm 0.15) \quad (1)$$

where the mean absolute magnitude of RR Lyrae stars has been derived from the Hipparcos observations and the slope of the M_v, $[Fe/H]$ relation from the Baade-Wesselink method.

Tsujimoto et al. (1998) and Luri et al. (1998) have determined the mean absolute magnitude from Hipparcos observations. They found $M_v(RR) \sim 0.6$ to 0.7 at $[Fe/H] = -1.6$ and $M_v(RR) = 0.65 \pm 0.23$ at $[Fe/H] = -1.51$, respectively. The differences between the different calibrations are usually less than 0.2 mag. However, Gratton et al. (1997) have used the subdwarf main-sequence fitting to derive the relation:

$$M_v = (0.22 \pm 0.09)([\mathrm{Fe/H}]{+}1.5) + (0.43 \pm 0.04) \quad (2)$$

which is about 0.3 mag brighter than that of Fernley et al. (1998). In this paper, we use the relation of Fernley et al. (1998) to derive the individual magnitudes. In Sect. 3.2, we discuss the influence on our results of the uncertainty in $M_v(RR)$. The Schlegel et al. (1998) all-sky reddening maps have been used to calculate the extinction on the position of each RR Lyrae star. Radial velocities and metallicities for these stars have been obtained from Fernley et al. (1998). The U, V, W components of the space velocities, where U is directed toward the Galactic center, V toward the Galactic rotation direction, and W toward the north Galactic pole, have been corrected for differential Galactic rotation. The Oort constants A = 14.4 km s^{-1} kpc $^{-1}$ and B = -12.0 km s^{-1} kpc $^{-1}$ are adopted (Kerr & Lynden-Bell, 1986).

3. The distribution of kinematics as a function of abundance

Since Gilmore & Reid (1983) proposed a galactic thick disk from a star count sample towards the south galactic pole, its existence and physical properties have been much discussed. From surveys of stellar proper motions and multicolor photometry, Robin et al. (1996) have suggested a separated galactic thick disk. On the other hand, Bahcall & Soneira (1984) used distributions in color and apparent magnitude of stars to set constraints on the galactic model parameters. They claimed that two components were sufficient to model the star count data without thick disk. Norris & Ryan (1991) found that relation between kinematics and abundance are better fitted by a 2-component model. They considered the thick disk as the high-velocity tail of the thin disk. Dawson (1986) has analyzed the LHS proper motion catalogue. His analysis showed that there is no significant local stellar population which has a kinematics intermediate between the old disk and the halo. Until now, it is still unclear whether a discrete thick disk population exists in the Galaxy.

3.1. Wavelet transform

The wavelet transform is one of the most useful methods for finding significant structures in a data set. An interesting astronomical application of wavelet transform is given by Chereul et al. (1998a,b), who used this technique to search for moving groups in the solar neighborhood. Another application provides a very nice description of all the structural components of the distribution of galaxy, such as clusters, filaments, voids (Slezak et al. 1990).

We have applied this method in the 2-dimensional space of velocity and metallicity (V, [Fe/H]). Before we carried out the wavelet analysis, we had to equalize the variables in an appropriate manner, which we did by taking a zero mean and unit standard deviation. The wavelet transform for the scale σ of the data is computed in each pixel (i, j) from the sample (δ_n, θ_n), n = 1, 2, 3,...144, according to:

$$W(i,j,\sigma) = \Sigma P(i-\delta_n, j-\theta_n) \quad (3)$$

with

$$P(x,y) = (2 - \frac{x^2+y^2}{2\sigma^2}) e^{-(x^2+y^2)/2\sigma^2} \quad (4)$$

The identification of structures in the data can be done at different scales (σ). However, for a very large σ value, the detailed structures in the data are smoothed, and for a very small σ, the fluctuations become important. In Fig. 2, we show the contour maps of the wavelet coefficients for different σ values. In Fig. 2c, we see three significant groups of data. For group 1, $(V, [Fe/H]) \sim (-10\,\mathrm{km\,s^{-1}}, -0.4\,\mathrm{dex})$, this is the disk population. From Figs. 2a and 2b, we also notice that this population contains two subgroups with different metallicities. We find that both subgroups have very similar kinematics (see Table 1). This leads us to conclude that the low metallicity part is the metal-weak tail of the disk stars and not a distinct population. Group 2 centered at $(V, [Fe/H]) \sim (-220\,\mathrm{km\,s^{-1}}, -1.6\,\mathrm{dex})$ belongs to the halo population. Between Group 1 and Group 2, we found an intermediate stellar population with $(V, [Fe/H])$ $\sim (-110\,\mathrm{km\,s^{-1}}, -1.3\,\mathrm{dex})$. This population can be identified at a different scale value (σ). From Figs. 2b and 2c, we can also see that the population of the halo stars in our sample may have substructure.

3.2. Kernel density estimation

The kernel density estimation is a powerful tool for identifying natural groups in data without assuming the forms of the distribution (Chen et al. 1997). The real probability density function

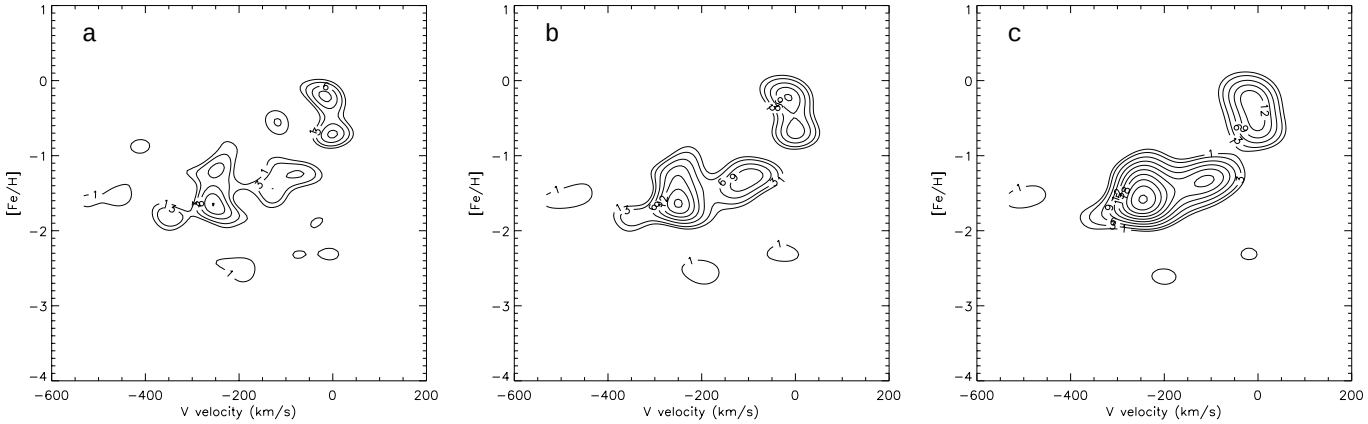

Fig. 2. a The contour map of the wavelet coefficients at σ = 0.3. **b** The contour map of the wavelet coefficients at σ = 0.4. **c** The contour map of the wavelet coefficients at σ = 0.5

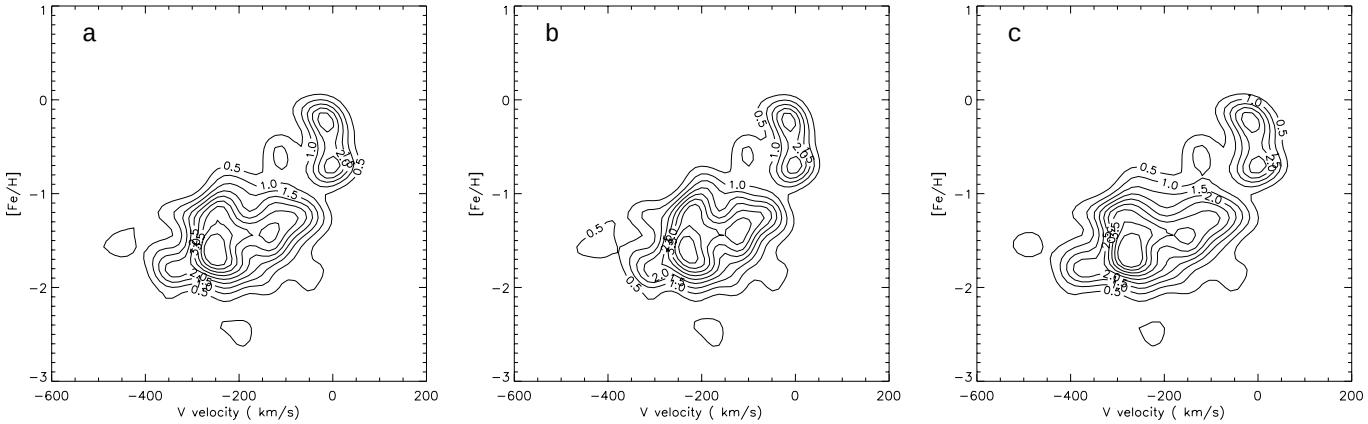

Fig. 3. a The contour map of the probability density function from the kernel density estimation for the real sample. **b** The contour map of the probability density function from the kernel density estimation for a 'pseudo-data' sample. **c** The contour map of the probability density function from the kernel density estimation using the $M_v - [Fe/H]$ relation of Gratton et al. (1997).

(pdf) p(x) for each star can be estimated by a kernel estimator $\hat{p}(x)$ of the density (Hand 1982):

$$\hat{p}(x_i) = \frac{1}{nh^d} \sum_{j=1}^{n} \frac{1}{|\Sigma|^{1/2}(2\pi)^{d/2}} e^{-\frac{1}{2h^2}(x_i - x_j)' \Sigma^{-1}(x_i - x_j)} \quad (5)$$

where x_i is the point at which the estimate is being made, n is the number of stars in the sample, x_j is the sample set defined in d-dimensional space $(x_i - x_j)$' is the transpose of the vector $(x_i - x_j)$ and Σ is the variance-covariance matrix of the sample.

The optimal smoothing parameter h derived by Silverman (1986) can be written as:

$$h = (\frac{4}{d+2})^{1/(d+4)} \sigma n^{-1/(d+4)} \quad (6)$$

where σ is the average marginal variance, $\sigma^2 = d^{-1}\Sigma\sigma_i^2$

From the definition of the kernel estimator, we know that it is the sum of multivariate normal density functions placed at the observations. The function determines the shape while the smoothing parameter h determines the width.

In Fig. 3a, we show the contour map obtained in the (V, $[Fe/H]$) space. We can see that the distributions are very similar to those derived from the wavelet transform: between galactic disk and halo stars, we can identify an intermediate galactic thick disk population.

In order to investigate the influence of the observational errors, we have generated a set of 'pseudo-data' samples. In each 'pseudo-data' sample, the original values of the parameters for each star have been randomly changed by assuming a normal distribution of errors with a zero mean and a standard deviation equal to the corresponding individual observational errors. We found that the observational errors do not change significantly the distribution of velocity as a function of abundance. For example, in Fig. 3b, we show one of the 'pseudo-data' samples. It can be seen that the main structure in the plane of (V, $[Fe/H]$) is not changed.

In order to investigate the influence of the uncertainty of $M_v(RR)$, we have used also the $M_v(RR) - [Fe/H]$ relation derived by Gratton et al. (1997). In Fig. 3c, we show the contour map in the (V, $[Fe/H]$) space. It can be seen that the kinematics for the disk population is not changed significantly because the distances to these stars are small. Changing the distance scale has a less pronounced effect on their calculated transverse

Table 1. The kinematical and chemical parameters of the three stellar populations in the sample.

	n	U	σ_U	V	σ_V	W	σ_W	[Fe/H]	$\sigma_{[Fe/H]}$
Disk stars	23	−18	33	−12	28	−18	22	−0.46	0.23
		(7)	(5)	(6)	(4)	(5)	(3)	(0.05)	(0.03)
Thick disk	37	−19	81	−106	68	6	75	−1.26	0.31
		(13)	(9)	(11)	(8)	(12)	(9)	(0.05)	(0.04)
Halo stars	84	−17	176	−254	87	2	90	−1.57	0.33
		(19)	(14)	(10)	(7)	(10)	(7)	(0.04)	(0.03)

velocities. However, this systematic uncertainty to the distance scale can cause significant changes in the mean velocities and dispersions for the halo and thick disk populations.

4. The kinematics of the RR Lyrae stars

The MIDAS multivariate data analysis package was used (Murtagh & Heck 1985) to isolate different stellar populations in an n-dimensional space. The clustering algorithm is based on a minimum within-class and maximum between-class variance principle (Chen 1996).

Because there is no systematic difference on the mean U and W velocity components between different stellar populations, U and W velocities are not good discriminant parameters for separating different populations. Instead, we use the residual velocities with respect to the Delhaye's (1965) centroid (9,12,7) km s^{-1}, $U_{res} = ((U-9)^2+(V-12)^2+(W-7)^2)^{1/2}$, as the discriminant parameter. Our cluster analysis has been carried out in the 3-dimensional space of (V, [Fe/H], U_{res}). Fig. 4 shows the upper part of the cluster merging hierarchy, together with the dissimilarity criterion, increasing from bottom to top. From Fig. 4, we see that the dissimilarity rises smoothly from nine clusters to three clusters, then it changes significantly from three clusters (0.12) to two clusters (0.37), indicating that there are three distinct clusters in our sample. This is in good agreement with our results from the kernel density estimation and the wavelet transform. In Table 1, we give the kinematical and chemical parameters of the three populations together with their size.

For the thin disk, we found a velocity dispersion (σ_U,σ_V, σ_W) = (33±5, 28±4, 22±3) km s^{-1}. Haywood et al. (1997) found 29.4±1.3, 24.9±1.1, 19.4±0.9 km s^{-1} respectively from a sample of G and K dwarfs observed by Hipparcos. Wielen et al. 1997 have used the RR Lyrae stars to study the transition from the halo to the disk. They found a velocity dispersion (σ_U,σ_V, σ_W) = (39±6, 30±5, 25±5) km s^{-1} for the disk stars. Both results are in good agreement with ours within the errors.

We found an average asymmetric drift of -106 ± 11 km s^{-1} and a metallicity [Fe/H] = −1.26 dex for the Galactic thick disk in our sample. Controversial results for the thick disk asymmetric drift and metallicity have been published in the literature. Layden et al. (1996) found a value of −48 km s^{-1}, Robin & Chen (1992) −80 km s^{-1}, and Wyse & Gilmore (1988) −100 km s^{-1}. Some studies have found average abundances of

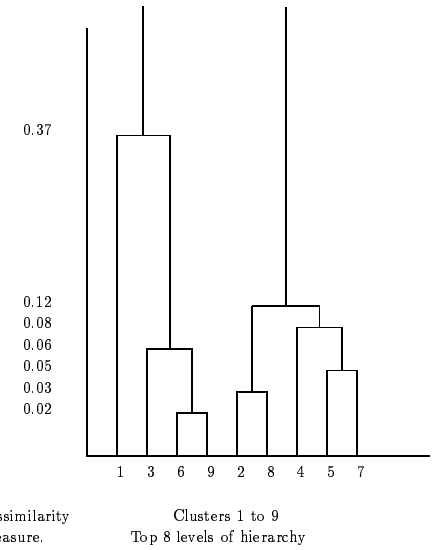

Fig. 4. The upper part of the cluster merging hierarchy for all stars in the sample. Dissimilarities are not drawn to scale.

[Fe/H] = −0.5 to −0.7 dex (Gilmore et al. 1995; Robin et al. 1996), with a significant low-metallicity tail extending to at least [Fe/H] ∼ −1.6 dex (Majewski 1993; Beers & Sommer-Larsen 1995). Morrison et al. (1990) suggested from their sample of red giants that there is a significant metal-weak thick disk (MWTD) component in their sample. Rodgers & Roberts (1993) also argued for a MWTD because they found a large number of candidate blue horizontal-branch stars. Layden (1995) found that a modest fraction of his sample of RR Lyrae stars show thick disk kinematics in the metallicity range $-1.3 \leq$ [Fe/H] ≤ -1. The differences in the characteristics of the thick disk found in the literature are due to the difficulties in separating the thick disk from other stellar populations. Different samples identify different part of the thick disk, thus may lead to different results.

We found an average asymmetric drift of -254 ± 10 km s^{-1} and a metallicity $[Fe/H]$ = −1.57 dex for the halo stars. The mean metallicity derived by us is in good agreement with the results of most previous investigations. For example, Saha (1985) and Carney et al. (1990) obtained mean values of [Fe/H] = −1.5 dex and −1.7 dex respectively. The asymmetric drift (V = −254 km s^{-1}) corresponds to a mean *retrograde* rotation of −34 km s^{-1}, if the local standard of rest (LSR) is rotating at 220 km s^{-1}. Conflicting results have been given for the asymmetric drift velocity of the Galactic halo. Results of halo kinematical studies (Ryan & Norris 1991, Carney & Latham 1986, Morrison et al. 1990) suggest that halo is in *prograde* rotation by many tens of km s^{-1}. Soubiran (1993) and Ojha et al. (1994) used star counts to derive the rotation velocity of the halo population. They found a *prograde* rotation velocity of 58 ± 12 km s^{-1} and 78 ± 8 km s^{-1}, respectively, while Reid (1990) and Majewski(1992) found that the halo is in *retrograde* rotation by 30 km s^{-1} and 55 km s^{-1} with respect to the disk from deep star count surveys. Recently, Majewski et al. (1996) found that a part of their sample (Majewski, 1992) in the North Galactic pole (NGP) field is a *retrograde* ($V \sim -340$ km s^{-1}) stellar

stream, and that the phase-space distribution of the halo stars has a significant structure. From our analysis with wavelet transform (see Fig. 2), we can see that a small group in halo stars has a large *retrograde* rotation velocity ($V = -350\,\mathrm{km\,s^{-1}}$). If we neglect these stars, we found a mean value of $V \sim -220\,\mathrm{km\,s^{-1}}$ with respect to the local standard of rest, implying no significant *prograde* or *retrograde* rotation for halo stars.

5. Discussion and conclusion

In this paper, we used RR Lyrae stars observed by Hipparcos to investigate the kinematics of stellar populations in the Milky Way. Recent magnitude calibration (Fernley et al. 1998) of RR Lyrae stars and an all-sky reddening map (Schlegel et al. 1998) have been used to derive individual distances accurately. The most important difference between this study and previous works (Wielen et al. 1997; Chiba & Yoshii 1998) is that we use three statistical methods well known in pattern recognition theory to search for significant signatures of stellar population characteristics in multivariate star count sample, to obtain information about structure otherwise unrecognizable, and to set important constraints on the space distribution of the different stellar populations in the Milky Way. All three methods (wavelet transform, kernel density estimation, multivariate cluster analysis) show that there is a separate galactic thick disk. This intermediate stellar population cannot be identified through a classical statistical analysis (for example the histogram of the V velocity).

Our results will help us to construct a detailed model of formation and evolution of the Milky Way. In the monumental work of Eggen et al. (1962), the proto-Galaxy was supposed to be metal-poor and spheroidal, and the Galaxy evolved rapidly and homogeneously into a smaller, rapidly-rotating, metal-rich disk. However, during the last two decades, many observations have suggested that the disk and halo are quite independent structures, probably with different formation histories. Recently, Majewski et al. (1996) and Chen (1998) have found that the Galactic halo is not dynamically mixed, suggesting that the disk and halo are completely separate kinematic structure without a smooth transition from one to the other. The present results support the conclusion of Majewski et al. (1996). These results suggest that the accretion of stellar aggregates plays an important part in the formation of the Galaxy. The existence of the Magellanic Stream and halo moving groups support these results – the breakup of stellar aggregates in the environment of the Milky Way. Moreover, galaxies may form by the coalescence of many subunits, which are presumably being continuously accreted by the enlarging galaxies.

Acknowledgements. I thank Drs. J. Torra, F. Figueras and X. Luri for some stimulating discussions. I thank Dr. Olivier Bienaymé for his critical reading of the manuscript and for useful suggestions. I am grateful to Dr. David Schlegel for making available to me the all-sky reddening map and for some discussions. This work has been supported by CICYT under contract PB95-0185, by the Acciones Integradas Hipano-Francesas (HF94/76B) and the Ministerio de Education y Ciencia.

References

Arenou F., Grenon M., Gómez A., 1992, A&A 258, 104
Bahcall J.N., Soneira R.M., 1984, ApJS, 55, 67
Beers T.C., Sommer-Larsen J., 1995, ApJS, 96, 175
Burstein D., Heiles C., 1982, AJ 87, 1165
Carney B.W., Aguilar L., Latham D.W., Laird J.B., 1990, AJ 99, 201
Carney B.W., Latham D.W., 1986, AJ 92, 60
Chen B., 1996, A&A 306, 733
Chen B., 1998, ApJ 495, L1
Chen B., Asiain R., Figuerea F., Torra J., 1997, A&A 318, 29
Chen B., Vergely J.-L., Valette B., Carraro G., 1998, A&A 336, 137
Chereul E., Crézé M., Bienaymé O., 1998a, A&AS 340, 384
Chereul E., Crézé M., Bienaymé O., 1998b, A&A in press (astro-ph/9809263)
Chiba M., Yoshii Y., 1998, AJ 115, 168
Dawson P.C., 1986, ApJ 311, 984
Delhaye J., 1965, In: Blaauw A., Schmidt M. (eds.) Galactic Structure. Univ. Chicago Press, Chicago, ch. 4
Eggen O.J., Lynden-Bell D., Sandage A.R., 1962, ApJ 136, 748
Fernley J., Barnes T.G., Skillen I., et al., 1998, A&A 330, 515
Gilmore G., Reid N., 1983, MNRAS 202, 1025
Gilmore G.F., Wyse R.F.G., Jones J.B., 1995, AJ 109, 1095
Gratton R.G., Fusi Pecci F., Carretta E., et al., 1997, ApJ 491, 749
Hand D.J., 1982, Kernel Discriminant Analysis. Research Studies Press, Chichester
Haywood M., Palasi J., Gomez A.E., Meillon L., In: Hipparcos Venice'97 Symp., ESA SP-402, 489
Kerr F.J., Lynden-Bell D., 1986, MNRAS 221, 1023
Kholopov P.N., 1985, General Catalog of Variable Stars. 4th Edition, Nauka Publishing House, Moscow
Layden A.C., 1995, AJ 110, 2312
Layden A.C., 1998, AJ 115, 193
Layden A.C., Hanson R.B., Hawley S.L., Klemola A.R., Hanley C.J., 1996, AJ 112, 2100
Luri X., Gómez A.E., Torra J., Figueras F., Mennessier M.O., 1998, A&A 335, L81
Majewski S.R., 1992, ApJS 78,87
Majewski S.R., 1993, ARA&A 31, 575
Majewski S.R., Munn J.A., Hawley S.L. 1996, ApJ 459, L73
Morrison H.L., Flynn C., Freeman K.C., 1990, AJ 100, 1191
Murtagh F., Heck A., 1985, Multivariate Data Analysis. D. Reidel Publishing Company
Norris J., Ryan S.G., 1991, ApJ 380, 403
Ojha D.K., Bienaymé O., Robin A.C., Mohan V., 1994, A&A 290, 771
Reid I.N., 1990, MNRAS 247, 70
Robin A.C., Chen B., 1992, Proceedings of the Third Annual October astrophysics in Maryland. College Park, Maryland
Robin A.C., Haywood M., Crézé M., Ojha D.K., Bienaymé O., 1996, A&A 305, 125
Rodgers A.W., Roberts W.H., 1993, AJ 106, 2294
Ryan S.G., Norris J.E., 1991, AJ 101, 1835
Saha A., 1985 ApJ, 289, 310
Schlegel D.J., Finkbeiner D.P., Davis M., 1998, ApJ 500, 525
Silverman B.W.,1986, In: Chapman and Hall (eds.) Density estimation for statistics and data analysis. Arrowsmith Ltd, Bristol
Slezak E., Bijaoui A., Mars G., 1990, A&A 227, 301
Soubiran C., 1993, A&A 274, 181
Tsujimoto T., Miyamoto M., Yoshii Y., 1998, ApJ 492, L79
Wielen R., Fuchs B., Dettbarn C., Jahreib H., Rockmann J., In: Hipparcos Venice'97 Symp., ESA SP-402, 639
Wyse R.F.G., Gilmore G., 1988, AJ 95, 1404